On transitions in the Schmidt number dependency of low solubility gas transfer across air-water interfaces

X.Yan[1], W. L. Peirson[2], J.W.Walker [3] and M. L. Banner[4]

[1] *Water Research Laboratory, School of Civil & Environmental Engineering, University of New South Wales, 110 King Street, Manly Vale, Sydney, Australia, E-mail: x.yan@wrl.unsw.edu.au*

[2] *Water Research Laboratory, School of Civil & Environmental Engineering, University of New South Wales, 110 King Street, Manly Vale, Sydney, Australia, E-mail: W.Peirson@wrl.unsw.edu.au*

[3] *Sogreah Gulf – Artelia Group, E-mail: james.WALKER@sogreah.ae*

[4] *School of Mathematics, University of New South Wales, Kensington, Sydney, Australia, E-mail: m.banner@unsw.edu.au*

Abstract. Local and global low solubility gas fluxes across air-water interfaces remain subject to significant uncertainty (Jähne *et al.* 2007). They are also of fundamental technological and environmental importance to: determining the spatial and temporal distribution of ocean atmospheric exchange of CO_2 and other climatically important gases; assessing the ecological integrity of open water bodies; and, assessment of key processes and cost of dissolved gases during water and wastewater treatment. Jähne and Haußecker (1998) show gradual change in the Schmidt number exponent characterizing the exchange behaviour as a function of friction velocity or mean squared slope of short wind waves in annular tanks. A study has been completed to determine the transition that occurs at the onset of wind waves in a linear tank with a clean interface. Ambient temperature was used to vary the Schmidt number of oxygen. Bulk concentration measurements of oxygen were used to determine the transfer velocity. Immediately prior to any transition (without any discernable wave activity) the Schmidt number exponent is determined to be approximately -0.62 and, at capillary ripple initiation, shifts to -0.47. These findings support previous experimental findings that the transition in Schmidt number occurs because of changes associated with the formation of surface waves. The transition is not associated with changes in surface active materials that might arrest free movement of the surface.

Key Words: Schmidt number exponent, low solubility gas transfer, temperature

1. Introduction

The exchange of low solubility gases between open water bodies and the atmosphere is a critical aspect of environmental science and engineering. Oceanic

gas exchange behaviour directly impacts large-scale climate, exchange in rivers and lakes, and is critical to the integrity of important aquatic systems. Aeration processes are fundamental to water and wastewater treatment.

Lewis and Whitman (1924) found that molecular diffusion sublayers are constrained to exist on each side of the air-water interface (Jähne and Haußecker, 1998, Figure 1). These diffusion sublayers control the rate of transfer from one phase to another. Mass transfer through each sublayer is proportional to the difference between the gas concentrations in the bulk outside and the interfacial concentration. The primary resistance to transfer of low solubility gases is offered by the aqueous diffusion sublayer. Consequently, the resistance contributed by the air-side diffusion sublayer is usually neglected in exchange studies of low solubility gases.

During this present experimental investigation, oxygen was selected as the tracer. This was because it is a representative low solubility gas (the solubility is 9.1mg/l at 20°C atmospheric pressure), a key gas of environmental concern in its own right and its use as a primary indicator of water quality and ecological integrity. Neglecting concentration gradients in the gas phase, the exchange rate of oxygen can be expressed as

$$j = K(C_I - C_L) \tag{1}$$

Where j is the flux of oxygen across the interface (kg/m^2·s); K is the transfer coefficient of the aqueous diffusion sublayer (m/s); C_I is the concentration of oxygen at the interface (kg/m^3); C_L is the concentration of oxygen in the bulk liquid (kg/m^3).

The quantity K, also known as the transfer velocity, is used to characterize the rate of absorption or evasion of oxygen. There are a number of potential factors that can affect the transfer velocity of oxygen including air water flow fields, surface contaminants, waves, turbulence and at higher levels of surface forcing, microscale breaking and bubble/droplet formation. Any factors that reduce the thickness of the diffusive sublayer will increase the transfer velocity. The broad range of potentially contributing factors has, to date, confounded development of an effective or universal model for K (Woodrow and Duke 2001). Consequently, parameterisations are used. The most widely used parameterisation is in the form (Deacon 1977):

$$K = \beta^{-1} Sc^{-n} u_{*w} \tag{2}$$

where the parameter β is the dimensionless transfer resistance for momentum transfer across the water-side viscous boundary layer (a form of Stanton number); Sc is the Schmidt number (the ratio of the water kinematic viscosity and the molecular gas diffusivity) with negative exponent n; and, u_{*w} is the friction

velocity in the water phase.

The parameter β and Schmidt number exponent depend on the surface wave field (Jähne *et al.* 1984). Using Reichardt's smooth solid wall boundary layer velocity profile as an analogy, Deacon (1977) determined $\beta=12$ and $n=2/3$ (for $Sc>10$). This has been shown to agree quite well at smooth water interfaces but significantly underestimate the transfer velocity with the onset of waves. Applying a Taylor expansion to the concentration profile near the interface, Ledwell (1984) showed that a shift in Schmidt number exponent from $-2/3$ for a smooth solid wall to $-1/2$ at a free surface. Coantic (1986) developed an identical result based on a slightly different reasoning but included comparison with available experimental results. Laboratory experiments carried out in circular tanks by Jähne and Haußecker (1998) verified the shift of Schmidt number exponent from $-2/3$ to $-1/2$ at low levels of wind forcing and mean squared slope. In an annular tank significant care was taken during the experiments to ensure that the interfacial conditions remain uncontaminated. Although, both theoretical and experimental studies have shown a shift in n, the character of the interfacial fluid mechanics has remained open to contention.

In parallel, other investigators have determined that the origin of these small interfacial waves is instabilities in the aqueous diffusion sublayer (Caulliez *et al*. 1997, Melville et al. 1997). Melville *et al.* (1997) further found that at very low wind speeds (3 to 5m/s) Langmuir circulations were also observed within wind-driven surface shear layer. These longitudinal counter-rotating vortices occur after initial wind wave-formation and cause larger-scale vertical mixing of the horizontal momentum which may enhance gas exchange at low wind speeds.

The purpose of this present investigation is to re-examine critically the mechanisms triggering the observed shift in the Schmidt number exponent. Laboratory experiments have been undertaken as they permit much greater control over the potentially confounding conditions described earlier. In this contribution, we summarise the experiments undertaken, discuss the results and make conclusions and recommendations on how this difficult problem is to be resolved.

2. Experiments

2.1 Experimental facility and surface conditions

The experimental procedure was designed to monitor the rate of gas exchange between atmosphere and water and employed two geometrically identical tanks with a variable wind speed at different temperatures. Temperature has been used to control the Schmidt number during the experiments: as temperature increases the water viscosity decreases and the molecular diffusivity of oxygen in water increases. The Schmidt number is determined using the method described by

Walker (2010) as follows. Diffusion coefficients of oxygen in water are based on those values tabulated in the CRC Handbook (2005). For the temperature not given in the handbook, the diffusion coefficients have been interpolated or extrapolated using a second order polynomial fit. The same approach has been applied to the viscosity of water.

Initial experiments were carried out in the same tank used by Walker and Peirson (2007) with an effective length of 3.12m, width of 0.245m and total height of 0.610m with a water depth of 250mm. Wind enters the tank smoothly from a mechanical fan. The tank was filled with clean water and, when not being used for experiments, the water was recirculated by a pump through a UV light unit and a diatomaceous earth filter. This was achieved by recirculating the tank water over a weir at the downwind end and capturing any surface material in the sump downstream of the weir. A light wind was applied to the water surface to encourage preferential transport of the surface microlayer over the weir and into the sump. The tank surface was visually examined to ensure that it remained clean. The tank is housed within an insulated room which can be temperature controlled to $\pm 0.5^{\circ}$C by means of air conditioner and varied over a temperature range of 17 to 28°C.

Unfortunately, our preliminary experiments showed that this temperature range provided insufficient variation in the Schmidt number (602 at 17°C, 308 at 28°C) in terms of maintaining a strong signal to noise ratio in our other measurements. Consequently, a smaller tank, whose total length equals the effective length of the tank used by Walker and Peirson (2007), with an identical fan, inlet flow arrangements and internal dimensions, was constructed. Preliminary testing was undertaken within the temperature controlled room to ensure that the bulk behaviour of the second tank was identical to the original. Once this was completed, the second tank was relocated to a cool room with a temperature set at 5°C, at which the Schmidt number of oxygen is 1317.

Two experimental conditions were investigated during this study. The first was with a wind speed of 2.1 m/s, which was the maximum wind forcing condition at 20°C for which no discernible waves were formed. The second was at a wind speed of 4.2m/s which was the lowest wind speed at which a consistent field of capillary ripples were observed to form over the entire surface of the tank, even at very short fetch. At 5°C, a similar field of capillary ripples was observed to form and capacitance wave probe measurements confirmed that the surface elevation variance σ of the two systems at different temperatures did not change by more than $\pm 0.4\%$. These observations are consistent with Jähne *et al*. (1979) who found that there was no significant effect of water temperature on waves at the same wind speed between 4°C and 20°C (in a nitrogen atmosphere and an annular tank).

Table 1 Experimental conditions in 2 tanks.

Surface condition	U_{10cm} (m/s)	u_{*w} (cm/s)	σ (mm)	Range of T (°C)	K (m/s) 18.8°C	$<n>$
Flat	2.1 (±0.4%)	0.43 (±0.01%)	–	5 to 28	9.965e−6 (±0.05%)	+0.62
Ripple covered	4.2 (±0.23%)	0. 63 (±0.25%)	0.34 (±0.4%)	5 to 28	1.601e−5 (±0.5%)	+0.47

Note: figures in brackets indicate the mean differences between the two tanks used during this study.

Wind speed and water friction velocity are derived from the air velocity profile above the water surface (Kawamura *et al*. 1981), which is measured by a pitot tube. The pitot tube was located at 2.4m fetch and the air velocity profile was measured as close as practical to the water surface.

A summary of the experimental conditions investigated is presented in Table 1.

2.2 Description of measurements

Oxygen concentration in the water was continuously measured with a flow-through oxygen probe (Microelectrodes Inc.) located at 20cm depth and 2.4m fetch. The probe was two-point calibrated at zero and saturation oxygen levels.

The time averaged mass transfer rate was obtained from the measurement of the change of oxygen concentration by transforming the flux rate (Equation 1) to a change in bulk concentration:

$$\frac{\partial C_L}{\partial t} = \frac{KA}{V}(C_I - C_L) \tag{3}$$

where V is the water volume and A is the surface area of water; C_L (mg/l) is the time-varying bulk oxygen concentration at time t; C_I (mg/l) is the saturation dissolved oxygen concentration at interface. After integration (Wolff and Hanratty, 1994),

$$K = \frac{-V}{At} ln \frac{C_I - C_L}{C_I - C_0} \tag{4}$$

where C_0 (mg/l) is the initial concentration. The transfer rate K is determined by least squares fitting of this model to the measured data. C_I is determined by the fitting procedure and reconciled against published values. For all experiments the fitted and published values are in agreement within one per cent.

Initially low dissolved oxygen concentrations were achieved by nitrogen stripping at the start of each experiment.

3. Results and discussion

Eighteen experiments were completed for the each of the characteristic water surface conditions at different ambient temperatures. An example of oxygen concentration time series and least-squares determination of K is shown is Figure 3.1.

For oxygen in water, Schmidt number decreases by a factor of 4 with an increase in temperature from 5°C to 28°C. The variation in gas transfer velocities

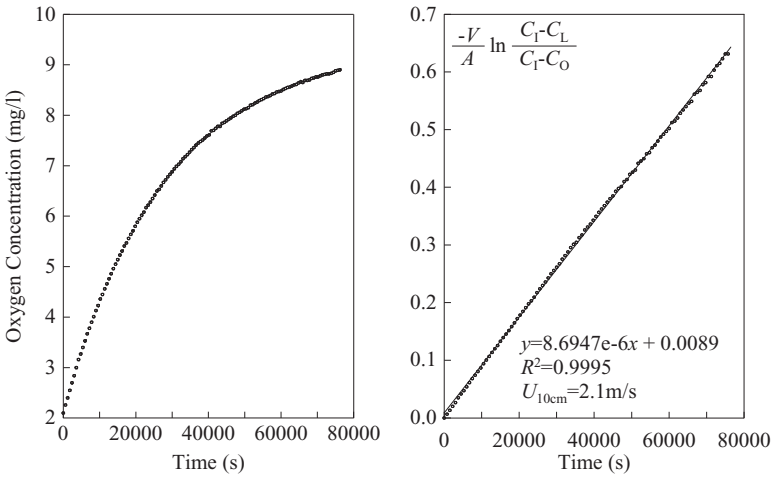

Figure 3.1 left: Oxygen concentration time series in flat water case at 18°C; right: least-squares fitting for K from equation(4)

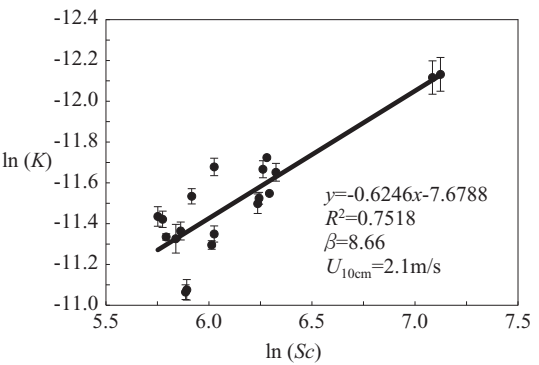

Figure 3.2 Natural logarithm of K as a function of the natural logarithm of the Schmidt number in the absence of wind-generated capillary ripples (flat interface).

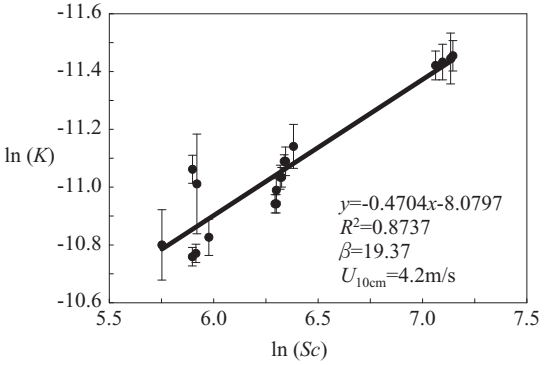

Figure 3.3 Natural logarithm of K as a function of the natural logarithm of Schmidt number in the presence of capillary ripples.

at different temperatures obtained from different wind speed is summarised as a function of *Sc* in Figure 3.2 and 3.3 for the two surface wave conditions. The uncertainty is the standard error in gradient determined from the Student ***t*** distribution assuming 90% level of confidence.

Transforming equation (1) to logarithmic quantities:

$$lnK = -nlnSc + \ln\frac{u_{*w}}{\beta} \tag{5}$$

and *n* can be determined from the slope of linear regression fits to the data in Figures 3.2 and 3.3.

It was found that the Schmidt number exponent transitions from a value of -0.62 to -0.47 with the onset of the capillary ripples. These measurements are placed in the context of the graphical summary of Jähne and Haußecker (1998) and shown in Figure 3.4. Measurements by Wanninkhof (1991) obtained at stronger levels of wave forcing have also been added.

The present measurements sit naturally amongst the Jähne and Haußecker (1998) data which is encouraging given the significant differences between the two test facilities (annular/linear) and the manner in which the Schmidt number exponent determinations have been made (gas pairs at a constant temperature/a single gas at different temperatures).

The theoretical work of Ledwell (1984) and Coantic (1986) predicted that this shift would occur due to changes in the interfacial boundary condition. However, our adopted methodology ensured removal of any surface active agents that would constrain fluctuating motions at the interface and our visual observations confirmed that these were not present.

At this point we are confronted with a fundamental theoretical gap in our

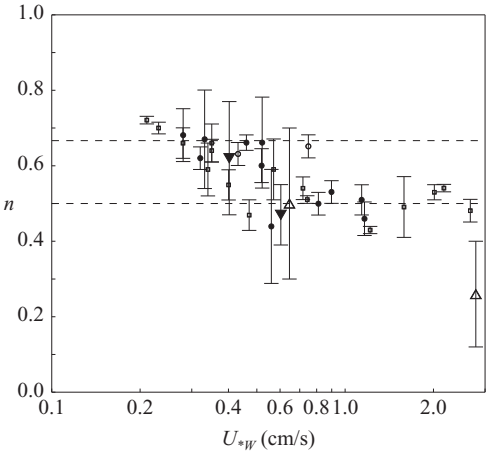

Figure 3.4 n as a function of water friction velocity. This figure is modified from Jähne and Haußecker (1998). Open circles, Jähne *et al*. (1998) smooth interface in small facilities; solid circles, Jähne *et al*. (1998) ruffled interface in small facilities; open squares, Jähne *et al*. (1998) ruffled interface in large facilities; open triangles, Wanninkhof *et al*. (1991) in a large linear tank using SF_6 and N_2O; downward pointing solid triangles, this study.

present understanding of the interface. Theoretical work by Csanady (1990) and Peirson and Banner (2003) predict that n will take a value of 0.5 but these predictions were formulated to address the condition of microscale breaking – a kinematic condition which is not observed at such weak levels of wind forcing. Whilst the theoretical work of Witting (1971), Macintyre (1971) and Szeri (1997) all predict enhancement of gas exchange in the presence surface waves, this is due to thinning of the aqueous diffusion sublayer by orbital straining. Witting (1971), Macintyre (1971) and Szeri (1997) do not predict any shift in the value of n.4. Conclusions.

In this investigation, temperature has been used to systematically vary the Schmidt number of oxygen and thereby determine the Schmidt number exponent of the aqueous diffusion sublayer transfer coefficient across the threshold of capillary ripple formation. This approach has been taken as an alternative to classical multiple tracer techniques. Even though this approach involves a bigger number of tests as a variety of temperature conditions are required, the present results provide a different perspective on this problem as only one tracer has been used. A further difference from previous measurements is that a linear tank rather than an annular tank has been used.

A confounding factor in such investigations can be contamination of the water

surface. In this study, tank conditions were carefully initiated to ensure any surface contamination was eliminated which might resist velocity fluctuations at the surface.

These experiments support the findings of Jähne and Haußecker (1998) that there is a significant shift in the Schmidt number exponent at the onset of surface waves. In these experiments, the Schmidt number exponent is found to be -0.62 for a flat interface under the maximum wind forcing that will generate no discernable wave activity. At the lowest level of wind forcing that will generate an approximately uniform field of capillary ripples, the Schmidt number exponent becomes −0.47. These values are in excellent quantitative agreement with Jähne and Haußecker (1998).

Theoretical explanations that rely on rigid and free interfacial motions to distinguish a shift Schmidt number exponent from −0.67 to −0.5 do not provide a theoretical explanation for this observation. Present theoretical descriptions of wave-enhanced gas exchange do not predict such a shift until microscale breaking is initiated.

Further work is required to explain these observations. Profile measurements within the aqueous viscous sublayer are recommended as a possible means of resolving the fundamental causes of this observed transition.

Laser Induced Fluorescent methods have been developed to probe the aqueous diffusion sublayer (Wolff and Hanratty 1994; Münsterer and Jähne 1998; Woodrow and Duke 2001; Walker and Peirson 2007) and presumably it is in this region the answer lies. However, Jähne and Haußecker (1998) report that distinguishing boundary layer models on the basis of aqueous diffusion sublayer concentration profiles is very difficult.

Another alternative is to critically examine the surface divergence behaviour of the free interface and reconcile the near-surface concentration profiles against the physical transport mechanisms that occur in this region. This was the theoretical approach of Coantic (1986) and should be possible with the near-surface Particle Image Velocimetry techniques developed by Peirson (1997). This course of investigation is presently being explored.

5. Acknowledgements

The authors gratefully acknowledge the assistance of Mr. John Hart and Mr. Robert Thompson who provided technical support and assistance during the course of this project.

References

Caulliez, G., Ricci, N. and Dupont, R. (1997) The genreration of the first visible wind

waves. Physics of Fluids, 10, 757-759.
Coantic, M. (1986) A model of gas transfer across air-water interfaces with capillary waves. Journal of Geophysical Research-Ocean,s 91, 3925-3943.
CRC (2005) CRC Handbook of chemistry and physics. 85th Ed.
Csanady, G.T. (1990) the role of breaking wavelets in air-sea gas transfer. Journal of Geophysical Research-Oceans, 95, 749-759.
Deacon, E.L. (1977) Gas transfer to and across an air-water interface. Tellus, 29:363-374.
Jähne, B. and Haußecker, H. (1998) Air-water gas exchange. Annual Review of Fluid Mechanics, 30, 443-468.
Jähne, B., Huber, W., Dutzi, A., Wais, T. and Ilmberger, J. (1984) Wind/wave-tunnel experiment on the Schmidt number-and wave field dependence of air/water gas exchange. Gas transfer at water surfaces, 303-309.
Jähne, B., Münnich, K.O. and Siegenthaler, U. (1979) Measurements of gas-exchange and momentum-transfer in a circular wind-water tunnel. Tellus, 31, 321-329.
Jähne, B., Popp, C., Schimpf, U. and Garbe, C.S. (2007) The influence of intermittency on air-water gas transfer measurements. Transport at the Air-Sea Interface: Measurements, Models and Parametrizations, 255-274.
Kawamura, H. Okuda, K., Toba Y. (1981) Structure of the turbulent boundary layer over wind waves in a wind tunnel. Journal of Tohoku Geophys, 28, 69-86.
Ledwell, J.R., (1984) The variation of the gas transfer coefficient with molecular diffusity Gas Transfer at Water surfaces., 293-302.
Lewis, W.K. and Whitman, W.G. (1924) Principles of gas absorption. Industrial and Engineering Chemistry, 16, 1215-1220.
Macintyre. F (1971) Enhancement of gas transfer by interfacial ripples. Physics of Fluids, 14, 1596-184.
Melville, W. K., Shear, R., Veron, F. (1997) Laboratory measurements of the generation and evolution of Langmuir circulations. J Fluid Mech., 364, 31-58.
Münsterer, T. and Jähne, B. (1998) LIF measurements of concentration profiles in the aqueous mass boundary layer. Experiments in Fluids, 25,190-196.
Peirson, W.L. (1997) Measurement of surface velocities and shears at a wavy air-water interface using particle image velocimetry. Experiments in Fluids, 23,427-437.
Peirson, W.L. and Banner, M. (2003) Aqueous surface layer flows induced by microscale breaking wind waves. J. Fluid Mech., 479, 1-38.
Szeri, A.J. (1997) Capillary waves and air-sea gas transfer. J Fluid Mech., 332:341-358.
Walker, J.W. and Peirson, W.L. (2007) Measurement of gas transfer across wind-forced wavy air-water interfaces using laser-induced fluorescence. Experiments in Fluids, 44, 249-259.
Walker, J.W.(2010) The exchange of oxygen at the surface of open waters under wind forcing. Ph.D. thesis, University of New South Wales, Australia.
Wanninkhof, R. (1991) Relationship between gas exchange, wind speed, and radar backscatter in a large wind-wave tank. Journal of Geophysical Research, 96, 2785-2796
Witting (1971) Effects of plane progressive irrotational waves on the thermal boundary layers. J Fluid Mech., 50,321-334
Wolff, L.M. and Hanratty, T.J. (1994) Instantaneous concentration profiles of oxygen absorption in a stratified flow. Experiments in Fluids., 16, 385-392
Woodrow, P.T. and Duke, S.R. (2001) Laser-induced fluorescence studies of oxygen transfer across unsheared flat and wavy air-water interfaces. Industrial and Engineering Chemistry Research 40, 1985-1995.